Coalescence of particles by differential sedimentation

P. Horvai, S.V. Nazarenko, and T.H.M. Stein*
University of Warwick, Mathematics Institute, CV4 7AL Coventry, United Kingdom

February 1, 2008

Abstract

We consider a three dimensional system consisting of a large number of small spherical particles, distributed in a range of sizes and heights (with uniform distribution in the horizontal direction). Particles move vertically at a size-dependent terminal velocity. They are either allowed to merge whenever they cross or there is a size ratio criterion enforced to account for collision efficiency. Such a system may be described, in mean field approximation, by the Smoluchowski kinetic equation with a differential sedimentation kernel. We obtain self-similar steady-state and time-dependent solutions to the kinetic equation, using methods borrowed from weak turbulence theory. Analytical results are compared with direct numerical simulations (DNS) of moving and merging particles, and a good agreement is found.

1 Introduction

We consider spherical particles in a viscous flow. The particles move vertically with their terminal velocity arising from the balance of the gravitational effect (fall or buoyancy) and viscous drag. Since, in general, particles of different sizes rise or fall with different velocities, their trajectories can cross and merging can happen. Realistic models of particle merging are quite involved and in the present text we are going to consider only two very simplified models: either any two particles whose trajectories cross merge, which we shall refer to as "free merging", or merging is restricted to particles of similar

*Electronic address: t.stein@warwick.ac.uk

sizes (i.e. small particles avoid big ones due to moving along flow streamlines bending around the big particle), which we call "forced locality" (defined in Sect. 2.3).

It will turn out that, although our problem is very simple to state, it is very rich in features. The simplified model can be realized by considering a sedimenting kernel in the Smoluchowski coagulation equation. We will derive solutions to this equation analytically, and we examine the validity of such solutions with direct numerical simulations (DNS), in which we let particles evolve individually according to certain rules for collisions and we study their overall size distribution. We shall study different stationary regimes, either in time t or in the vertical coordinate z, and we will discuss self-similar solutions and study the role of local and non-local merging. Whereas time dependent solutions of the sedimenting kernel have received a lot of attention in the literature [1, 2, 3], the study of height dependence – also treated here – is more rare.

The process we discuss is usually referred to as differential sedimentation and has been linked to experimental results [4] and is used to predict rain initiation time [5, 6]. In particular, the model admits a power law distribution consistent with experimental data for aerosols [5]. In our discussion, we will obtain this power law as an exact result, rather than by dimensional analysis used in previous discussions [4, 7]. We recognize this result as a Kolmogorov-Zakharov (KZ) cascade of the volume integral, similar to the solutions that arise in wave turbulence. Solutions to the coagulation equation with a KZ cascade have been studied in general [8, 9], and with a kernel describing galaxy mergers in particular [10].

We find that in the free-merging model the locality assumption necessary in dimensional analysis and the KZ spectrum fail to hold [8]. We will obtain an analytical solution for such a non-local system, and verify this with DNS. We will study self-similarity for both the forced-locality model and the free-merging model. We will perform DNS for inhomogeneous solutions that are self-similar in the spatial variable z.

The starting point of our analysis is to write a kinetic equation for the coagulation process in Sect. 2.1. In Sect. 3 we find the Kolmogorov-Zakharov solution for the kinetic equation. Sect. 4 discusses the dominance of non-local interactions in the system. We study self-similarity of our model in Sect. 5, and we analyze locality of such solutions in Sect. 6, where we present numerical data. Finally, we introduce a "super-local" model in Sect. 7, reducible to Burgers equation.

2 The model

Let us denote by σ the volume of a spherical particle and by r its radius,

$$\sigma = \kappa r^3 \ , \qquad \kappa = 4\pi/3 \ . \tag{1}$$

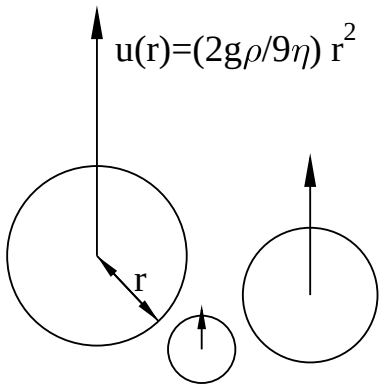

Figure 1: A particle's terminal velocity u is determined by its radius r. Larger particles will have a larger terminal velocity, depicted by the arrows, following definition (2). (Created by T.H.M.Stein)

The Stokes terminal velocity of a rigid sphere of radius r with no slip boundary conditions is given by the formula [11, 5, 12]

$$u(r) = cr^2 \ , \qquad c = \frac{2g(\rho_f - \rho_p)}{9\eta_f} \ , \tag{2}$$

where g is the free fall acceleration, ρ_f and ρ_p are the density of the surrounding fluid and the particle respectively, and η_f is the dynamic viscosity of the surrounding fluid.

Experimentally, the formulae (2) are valid for air bubbles in water at 20°C with $r < 1$mm, and these bubbles can be considered spherical. Slip-flow corrections can be necessary for other gases and fluids [12]. The following data for water droplets and particles in the atmosphere can be found in Pruppacher and Klett [5]. For droplets, corrections to (2) are necessary when $r > 30\mu$m, which changes the formula's dependence on r^2. They can be considered spherical for radii up to 535μm. For atmospheric particles, (2) can be considered to depend on r^2 for large particles. However, atmospheric particles are generally not spherical and will thus require other corrections.

Despite physical complications, we will assume (2) and (1), and we will express both in terms of volume σ,

$$r(\sigma) = \kappa^{-1/3}\sigma^{1/3} \ , \qquad u(\sigma) = c\kappa^{-2/3}\sigma^{2/3} \ . \tag{3}$$

We compute this model using direct numerical simulations in a periodic box of $10 \times 10 \times 10$cm with particles that are defined by their x-, y-, and z-coordinates and by their volume σ. At each time step the particles move according to their fixed terminal velocity, using definition (2). We fix our parameter c such that a particle of radius 0.1cm moves upwards with velocity 20cms^{-1}, which resembles the situation of air bubbles in water [12].

The particles are generated at a range of small σ, with their smallest volume $\sigma_0 \approx 4.2 \cdot 10^{-6}\text{cm}^3$, equivalent to a radius $r = 0.01$cm. They are removed from the system once they become larger than $10^3\sigma_0$, or $r \sim 1$mm and are assumed to be spherical at all sizes for computational purposes. With different velocities, the particle trajectories may cross, and depending on the rules of interaction they can then merge. These rules are governed by collision efficiency, which will be explained in Sect. 2.1.

2.1 The kinetic equation

We suppose that the distribution of particles can be adequately characterized by density $n(\sigma, z, t)$ (the number of particles N of volume between σ and $\sigma + \mathrm{d}\sigma$, per fluid volume V per $\mathrm{d}\sigma$, at the vertical coordinate z and at instant t). In particular we suppose here that the dependence of particle distribution on the horizontal coordinates can be averaged out. This hypothesis is valid if the dynamics do not lead to strongly intermittent distribution in the horizontal directions, for example if the fluid is well mixed in the horizontal directions. Our numerical simulations appear to support such a mean field approach well, and in future work it would be interesting to examine theoretically why this is the case.

The goal of this section is to derive a kinetic equation for n – also called Smoluchowski coagulation equation [13] – using a kernel describing differential sedimentation. We write the collision integral, which expresses simply the fact that two particles of volumes σ_1 and σ_2, with $\sigma_1 + \sigma_2 = \sigma$, can merge to give a particle of volume σ (inflow), or a particle with volume σ can merge with any other particle of volume $\sigma_1 > 0$ and give a particle with volume $\sigma_2 = \sigma + \sigma_1$ (outflow). Also, we determine the cross-section of interaction between two particles by the condition that particles merge upon touching, that is if their centers are at a distance at most $r_1 + r_2$, which gives the geometric cross-section of $\pi(r_1 + r_2)^2$. Finally the collision rate between particles

of volume σ_1 and σ_2 is taken to be proportional to their relative velocities $|u(\sigma_1)-u(\sigma_2)|$ and to their number densities n_1 and n_2, which is a mean field type hypothesis.

The left hand side of the kinetic equation contains the advection term $\partial_t n + u\partial_z n$, which we shall also denote as the total derivative $\mathrm{d}n/\mathrm{d}t$, while on the right hand side we put the collision integral. Note also the shorthand $n = n(\sigma, z, t)$, $u = u(\sigma)$, $n_1 = n(\sigma_1, z, t)$, $u_1 = u(\sigma_1)$, $r_1 = r(\sigma_1)$ and similar for n_2, u_2 and r_2. Thus we find

$$\begin{aligned}\partial_t n + u\partial_z n = & \\ &+\frac{1}{2}\int_0^{\sigma} \mathrm{d}\sigma_1\mathrm{d}\sigma_2\,|u_2-u_1|\pi(r_1+r_2)^2 n_1 n_2\delta(\sigma-\sigma_1-\sigma_2) \\ &-\frac{1}{2}\int_0^{+\infty} \mathrm{d}\sigma_1\mathrm{d}\sigma_2|u-u_2|\pi(r+r_2)^2 n n_2\delta(\sigma_1-\sigma-\sigma_2) \\ &-\frac{1}{2}\int_0^{+\infty} \mathrm{d}\sigma_1\mathrm{d}\sigma_2|u-u_1|\pi(r+r_1)^2 n n_1\delta(\sigma_2-\sigma-\sigma_1)\ .\end{aligned} \tag{4}$$

It is useful to express the u and r in terms of σ using (3),

$$\begin{aligned}\partial_t n + c\kappa^{-2/3}\sigma^{2/3}\partial_z n = & \\ \frac{c\kappa^{-4/3}\pi}{2}\int_0^{+\infty}\mathrm{d}\sigma_1\int_0^{+\infty}\mathrm{d}\sigma_2\ & |\sigma_2^{2/3}-\sigma_1^{2/3}|(\sigma_1^{1/3}+\sigma_2^{1/3})^2 n_1 n_2\delta(\sigma-\sigma_1-\sigma_2) \\ &-|\sigma^{2/3}-\sigma_2^{2/3}|(\sigma^{1/3}+\sigma_2^{1/3})^2 n n_2\delta(\sigma_1-\sigma-\sigma_2) \\ &-|\sigma^{2/3}-\sigma_1^{2/3}|(\sigma^{1/3}+\sigma_1^{1/3})^2 n n_1\delta(\sigma_2-\sigma-\sigma_1)\ .\end{aligned} \tag{5}$$

Let us introduce the interaction kernel $K(\sigma_1, \sigma_2)$,

$$K(\sigma_1,\sigma_2) = \frac{c\kappa^{-4/3}\pi}{2}|\sigma_2^{2/3}-\sigma_1^{2/3}|(\sigma_1^{1/3}+\sigma_2^{1/3})^2\ , \tag{6}$$

which for a general kernel K reduces Eq. (4) to the Smoluchowski equation. It is useful to note that our kernel (6) is homogeneous in σ, with $K(\zeta\sigma_1, \zeta\sigma_2) = \zeta^{4/3}K(\sigma_1, \sigma_2)$. We also introduce the collision rates

$$R_{\sigma 12} = K(\sigma_1,\sigma_2)n_1 n_2\delta(\sigma-\sigma_1-\sigma_2) \tag{7}$$

with $R_{1\sigma 2}$, $R_{2\sigma 1}$ defined analogously. Now the RHS of Eq. (5) can be written in a compact form

$$\frac{\mathrm{d}n}{\mathrm{d}t} = \int_0^{+\infty}\mathrm{d}\sigma_1\int_0^{+\infty}\mathrm{d}\sigma_2\,(R_{\sigma 12}-R_{1\sigma 2}-R_{2\sigma 1})\ . \tag{8}$$

2.2 Characteristic timescales

We study the physical relevance of Eq. (5) by comparing its characteristic time τ_{ds} with the characteristic residence time in a typical system, $\tau_g = L/u$, where L is the vertical extent of the system, and u is as in Eq. (3). To find τ_{ds}, we note that $n \sim \frac{N}{\sigma V}$ and we introduce the volume fraction $v \sim \frac{N\sigma}{V}$, so that:

$$n \sim \frac{v}{\sigma^2} \ .$$

Now, using the kinetic equation (5) we can write

$$\frac{1}{\tau_{ds}} = c\kappa^{-4/3}\pi\sigma^{2+2/3+2/3-1}\frac{v}{\sigma^2} = c\kappa^{-4/3}\pi\sigma^{1/3}v \ . \tag{9}$$

Thus we find the following relation between the characteristic times:

$$\frac{\tau_g}{\tau_{ds}} = \frac{Lc\kappa^{-4/3}\pi\sigma^{1/3}v}{c\kappa^{-2/3}\sigma^{2/3}} \approx \frac{2L}{r}v \ , \tag{10}$$

where we recall that $\sigma^{1/3} = \kappa^{-1/3}r$ and approximate $\kappa^{-1/3}\pi \approx 2$. From [5] we find that for a cumulus cloud, typically $L \sim 10^3$m, $r \sim 10^{-5}$m, and $v \sim 10^{-6}$. Thus, we find that $\tau_g/\tau_{ds} \sim 10^2$, which implies that the kinetic equation is relevant in a cloud system with gravity when we regard time and length scales.

2.3 Collision efficiency

The kinetic equation (5) allows merging of particles of any sizes, without any discrimination. We shall refer to this case as "free merging". More realistically one should also take into account the collision efficiency between particles. We define collision efficiency $\mathcal{E}_{12} = \mathcal{E}(\sigma_1, \sigma_2)$ between particles of volumes σ_1 and σ_2 as a number between 0 and 1, which enters the collision integral by multiplication with the collision rates R, so $R_{\sigma 12}$ would be replaced by $R_{\sigma 12}\mathcal{E}_{12}$ and more generally for example the integrand of Eq. (8) would become $R_{\sigma 12}\mathcal{E}_{12} - R_{1\sigma 2}\mathcal{E}_{\sigma 2} - R_{2\sigma 1}\mathcal{E}_{\sigma 1}$.

In particular, one could restrict merging to particles of similar sizes, taking into account that small particles cannot collide with much larger ones because they bend around them along the fluid streamlines. In the simplest such model which will be considered later in this paper,

$$\mathcal{E}_{12} = \begin{cases} 1 & \text{if } 1/q < \sigma_1/\sigma_2 < q, \\ 0 & \text{otherwise,} \end{cases} \tag{11}$$

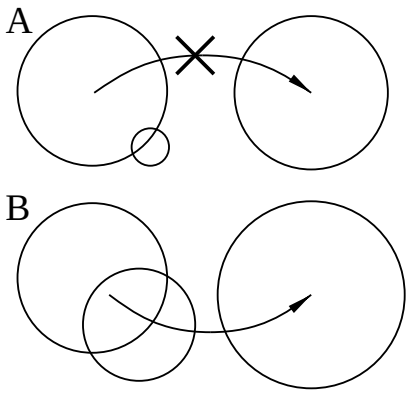

Figure 2: Without applying the efficiency kernel $\mathcal{E}$, particles merge whenever they cross. Including $\mathcal{E}$ with small q, only situation B is allowed, i.e. only particles of similar size may merge; particles of dissimilar size (situation A) are allowed to cross one another without merging. (Created by T.H.M.Stein)

where $q > 1$ is the number representing the maximal volume ratio for the particle merging. Compared to a more involved form of collision efficiency used by Valioulis et al. [14], the simplified kernel we use mimics the behavior for particles with $r = 0.01$cm which is similar to the regime we study numerically. We will refer to the model with finite q as "forced locality".

2.4 Scaling argument

For our simple setup one could derive a steady state solution merely by physical and dimensional arguments, following Friedlander [15], Jeffrey [7], and Hunt [4]. The main remark is that at steady state, the system has a constant flux of volume. The total volume of particles per unit volume of fluid that passes from particles smaller than σ to particles greater than σ is of the order:

$$\int_{\sigma}^{2\sigma} \frac{\mathrm{d}n}{\mathrm{d}t} s \mathrm{d}s \ . \tag{12}$$

We can estimate from the kinetic equation (8) and equations (7) and (6) that $\mathrm{d}n/\mathrm{d}t \sim \sigma^2 R$, with $R \sim K n^2 \sigma^{-1}$ and $K \sim \sigma^{4/3}$. If we assume that $n \sim \sigma^{\nu}$, we find that $\mathrm{d}n/\mathrm{d}t \sim \sigma^{7/3+2\nu}$, and we obtain the scaling $\sigma^{13/3+2\nu}$ for the volume flux (12). For constant flux, we arrive at $\nu = -13/6$, or $n \sim \sigma^{-13/6}$. Naturally, the dimensional analysis assumes locality of interactions.

3 Kolmogorov-Zakharov solution

One of the simplest questions one can ask with respect to the kinetic equation (5) is if it allows for a scaling stationary solution of non-zero flux. Such a solution, if one exists, is called a Kolmogorov-Zakharov (KZ) spectrum because, like in the classical Kolmogorov spectrum, it corresponds to a cascade of a conserved quantity (total volume occupied by particles in our case) [8, 10]. In this section we investigate the scaling exponent and existence of such solutions.

3.1 Zakharov transform

A derivation of the KZ solution can be achieved through the technique of the Zakharov transform [8, 16]. Let us consider a steady state (i.e. time and space independent) solution of Eq. (5) of form $n \sim \sigma^\nu$, and let us aim to find ν. Note that this is a reasonable thing to look for, since we can easily see from Eq. (5) that our collision integral is a homogeneous function in the σ and in the n.

We start by expanding our collision rates from equation (7) using equation (6), and obtain the following equation in σ:

$$R_{\sigma 12} = \frac{c\kappa^{-4/3}\pi}{2}|\sigma_2^{2/3} - \sigma_1^{2/3}|(\sigma_1^{1/3} + \sigma_2^{1/3})^2\sigma_1^\nu\sigma_2^\nu\delta(\sigma - \sigma_1 - \sigma_2)$$

where $R_{1\sigma 2}$ and $R_{2\sigma 1}$ are expanded similarly. We then continue by non-dimensionalising the rates R by writing σ_1 as $\sigma_1'\sigma$ and σ_2 as $\sigma_2'\sigma$, so

$$R_{\sigma 12} = \frac{c\kappa^{-4/3}\pi}{2}\sigma^{1/3+2\nu}|\sigma_2'^{2/3} - \sigma_1'^{2/3}|(\sigma_1'^{1/3} + \sigma_2'^{1/3})^2\sigma_1'^{\nu}\sigma_2'^{\nu}\delta(1 - \sigma_1' - \sigma_2') \tag{13}$$

and $R_{1\sigma 2}$ and $R_{2\sigma 1}$ are transformed in a similar way.

The Zakharov transform consists in passing in $R_{1\sigma 2}$ to new variables $\tilde{\sigma}_1$ and $\tilde{\sigma}_2$ defined by

$$\sigma_1' = \frac{1}{\tilde{\sigma}_1}\ , \qquad \sigma_2' = \frac{\tilde{\sigma}_2}{\tilde{\sigma}_1}\ .$$

This way, we obtain

$$R_{1\sigma 2} = \frac{c\kappa^{-4/3}\pi}{2}\sigma^{2\nu+1/3}\tilde{\sigma}_1^{-1/3-2\nu}|\tilde{\sigma}_2^{2/3} - \tilde{\sigma}_1^{2/3}|(\tilde{\sigma}_1^{1/3} + \tilde{\sigma}_2^{1/3})^2\tilde{\sigma}_2^\nu\tilde{\sigma}_1^\nu\delta(1 - \tilde{\sigma}_1 - \tilde{\sigma}_2)\ . \tag{14}$$

A similar expression is derived for $R_{2\sigma 1}$.

Combining the transformed terms and dropping primes and tildes, we transform the compact kinetic equation (8)

$$0 = \int_0^{+\infty} \mathrm{d}\sigma_1 \int_0^{+\infty} \mathrm{d}\sigma_2 \; (1 - \sigma_1^{-10/3-2\nu} - \sigma_2^{-10/3-2\nu}) R_{\sigma 12} \; .$$

Here, we note that the integration variables for $R_{1\sigma 2}$ become $\mathrm{d}\sigma_1 \mathrm{d}\sigma_2 = \sigma^2 \tilde{\sigma}_1^{-3} \mathrm{d}\tilde{\sigma}_1 \mathrm{d}\tilde{\sigma}_2$, with a similar transformation in $R_{2\sigma 1}$. Now, if we choose ν such that $-10/3 - 2\nu = 1$, then we have the factor $\delta(1-\sigma_1-\sigma_2)(1-\sigma_1-\sigma_2) = 0$ appearing in the integrand, which solves the equation, i.e. $\nu = -13/6$ is the candidate for the KZ exponent. This method of derivation can be applied to various kernels for the Smoluchowski equation [8].

Let us note that our exponent ν is that of $n(\sigma)$. In literature, one commonly finds the radius distributions, $n(r)$, which can be expressed in terms of $n(\sigma)$ from the relationship $n(\sigma)\mathrm{d}\sigma = n(r)\mathrm{d}r$. Thus, $n(r) = n(\sigma)\mathrm{d}\sigma/\mathrm{d}r \propto r^{3\nu} r^2 = r^{3\nu+2}$, and therefore $\nu_r = 3\nu + 2 = -9/2$ [7].

However, the KZ spectrum is only a true solution of Eq. (5) if the collision integral on the RHS of this equation (prior to the Zakharov transformation) converges. This property is called locality, and it physically means that the particle kinetics are dominated by mergings of particles with comparable (rather than very different) sizes. Convergence of the collision integral on general power-law distributions will be studied in Appendix A. We will see that (without modifying the model to enforce locality) the $-13/6$ scaling exponent gives rise to non-local interaction between the particles both with the smallest and the largest particles and, therefore, the KZ spectrum is not a valid solution in this case.

3.2 KZ spectrum in the system with forced locality

Locality of interactions, and therefore validity of the KZ solution, are immediately restored if one modifies the model by introducing the local collision efficiency kernel as in definition (11). This kernel is a homogeneous function of degree zero in σ and, therefore, the KZ exponent obtained via the Zakharov transformation remains the same. In Fig. 3 we can see that the Kolmogorov-Zakharov scaling appears in a system with forced locality.

4 Kinetics dominated by non-local interactions

As an alternative, we may assume that the dominant interactions are non-local and find a cut-off dependent stationary solution. This is relevant if it is

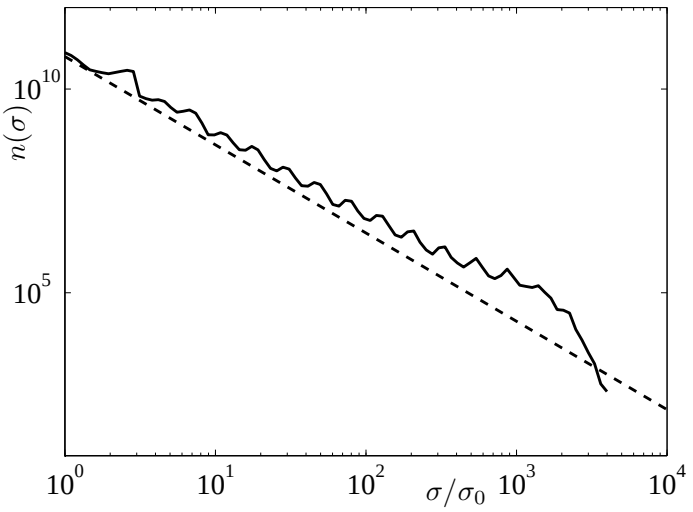

Figure 3: Distribution of particle volumes averaged over several times after 140,000 time steps for the forced locality situation with $q = 2$. The dashed slope represents the $-13/6$ KZ spectrum (compare with [14]).

not desirable to use the collision efficiency models which guarantee locality (for instance using the kernel (11)). In this case one should accept the fact the kinetics are dominated by non-local interactions, and that the low-σ or/and high-σ cut-offs dominate the collision integral. In fact, such a non-locality can allow us to significantly simplify the kinetic equation and reduce it to a differential equation form. As shown in Appendix A, contribution to the collision integral from non-local interactions with the smallest particles ($\sigma_1 \ll \sigma$) is

$$- c_1 \partial_\sigma (\sigma^{4/3} n) \ , \qquad \text{where} \qquad c_1 = \int_{\sigma_{\min}} n_1 \sigma_1 \mathrm{d}\sigma_1 \ . \tag{15}$$

where we have dropped the explicit dependence of the upper integration limit on σ, since the integral is divergent as $\sigma_{\min} \to 0$ (this is the hypothesis of non-locality), so the dependence on the upper bound is a sub-dominant contribution.

The contribution to the collision integral from non-local interactions with the largest particles ($\sigma_1 \gg \sigma$) is

$$- c_2 n \ , \qquad \text{where} \qquad c_2 = \int^{\sigma_{\max}} n_1 \sigma_1^{4/3} \mathrm{d}\sigma_1 \ . \tag{16}$$

Similarly to above, here the lower integration bound is omitted.

Putting these two formulae together, we obtain the following effective kinetic equation for the cases when the non-local interactions are dominant,

$$\frac{\mathrm{d}n}{\mathrm{d}t} = -c_1 \partial_\sigma (\sigma^{4/3} n) - c_2 n \ , \tag{17}$$

where constants c_1, c_2 are defined in the formulae (15) and (16). Note that this equation (17) is valid when the non-local interactions with the smallest and with the largest particles give similar contributions, as well as in cases when one type of non-locality is dominant over the other.

In steady state $\mathrm{d}n/\mathrm{d}t = 0$ and the solution of the resulting ordinary differential equation is

$$n = C\sigma^{-4/3} e^{\frac{3c_2}{c_1}\sigma^{-1/3}} \ , \tag{18}$$

with C being an arbitrary positive constant. Note that the constants C and c_2/c_1 appearing in the solution (18) can be related to the "physical" data of $\sigma_{\min}$, $\sigma_{\max}$ and $n(\sigma_{\min})$, through Eqs. (15), (16) and (18). We obtain

$$n(\sigma) = n(\sigma_{\min}) \frac{\exp\left[\left(\frac{\sigma}{\sigma_{\min}}\right)^{-1/3} \log \frac{\sigma_{\max}}{\sigma_{\min}}\right]}{\left(\frac{\sigma}{\sigma_{\min}}\right)^{4/3} \frac{\sigma_{\max}}{\sigma_{\min}}} \ . \tag{19}$$

The solution (18) is interesting since it is not a pure power law. For large σ we have $n \sim C\sigma^{-4/3}$ which is a limit when absorption of the smallest particles is much more important than being absorbed by the large particles, i.e. when the first term on the LHS of Eq. (18) is much greater than the second one. This limit corresponds to a cascade of the number of particles (not their volume!) which is a conserved quantity in this regime.

In Fig. 4 we show our numerical results for the non-local model. Particles are produced uniformly in space with volumes ranging from σ_0 to $3\sigma_0$, and particle density within this size range is kept constant in time. Particles are removed from the system once they reach $\sigma_{\max} = 10^3\sigma_0$, with probability $p(\sigma) = 1 - \exp^{-a(\sigma-\sigma_{\max})^4}$ with $a \ll 1$. The original results have been averaged over neighbouring data points to obtain the continuous graph in Fig. 4. We also used Eq. (19) and find that with appropriate parameters this solution fits the numerical data.

We can check our hypothesis of dominance of non-local interactionsdirectly by counting the number of collisions within a certain timeframe at statistical steady state. Namely, for each size bin we count the number of collisions leading to a particle entering the bin, and the number of collisions leading to a particle leaving the bin. We distinguish between local and

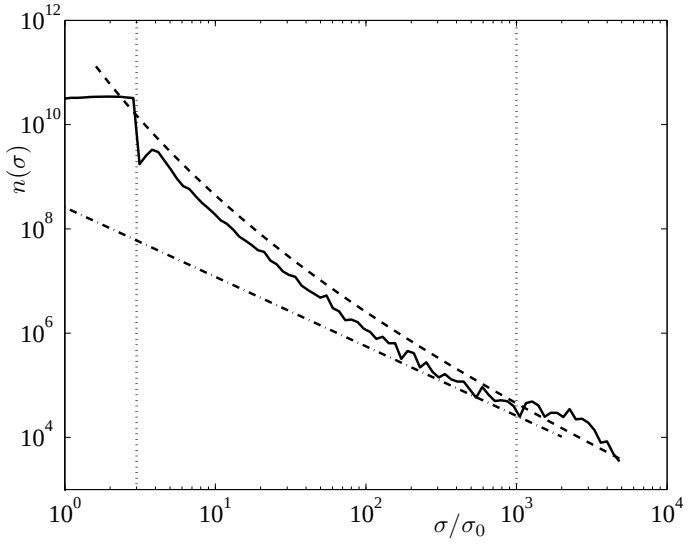

Figure 4: Averaged distribution of particle sizes for the situation without forced locality ("$q = \infty$") after 200,000 time steps. The vertical dotted lines bound the inertial range at $\sigma_{\min} = 3\sigma_0$ and $\sigma_{\max} = 10^3\sigma_0$. The dashed curve represents the fit conform eq. (19), with $\sigma_{\min}$ and $\sigma_{\max}$ given by the bounds of the inertial range, and $n(\sigma_{\min}) = 1.5 \cdot 10^{10}$; the dash-dot slope represents a power law of $\sigma^{-4/3}$.

non-local collisions using the particle size ratio q^*, i.e. if $1/10 < q^* < 10$ we consider the collision local, and non-local otherwise. For non-local collisions, we distinguish between a collision with a very large particle and a very small particle. In the kinetic equation (5) (which we do not rely on in our procedure) this would correspond to splitting the collision integral as follows:

$$\begin{aligned}\frac{\mathrm{d}n}{\mathrm{d}t} = &+ \int_{\sigma_{\min}}^{\sigma/q} \mathrm{d}\sigma_1 f(\sigma_1, \sigma - \sigma_1) - \int_{\sigma_{\min}}^{\sigma/q} \mathrm{d}\sigma_1 f(\sigma_1, \sigma) \\ &+ \int_{\sigma/q}^{\sigma/2} \mathrm{d}\sigma_1 f(\sigma_1, \sigma - \sigma_1) - \int_{\sigma/q}^{q\sigma} \mathrm{d}\sigma_1 f(\sigma_1, \sigma) \\ &- \int_{q\sigma}^{\sigma_{\max}} \mathrm{d}\sigma_1 f(\sigma_1, \sigma)\end{aligned} \tag{20}$$

where

$$f(\sigma_1, \sigma_2) = K(\sigma_1, \sigma_2) n_1 n_2 \ .$$

We perform DNS and for each collision that occurs we count its contribution to the different collision regimes as mentioned above. Our results

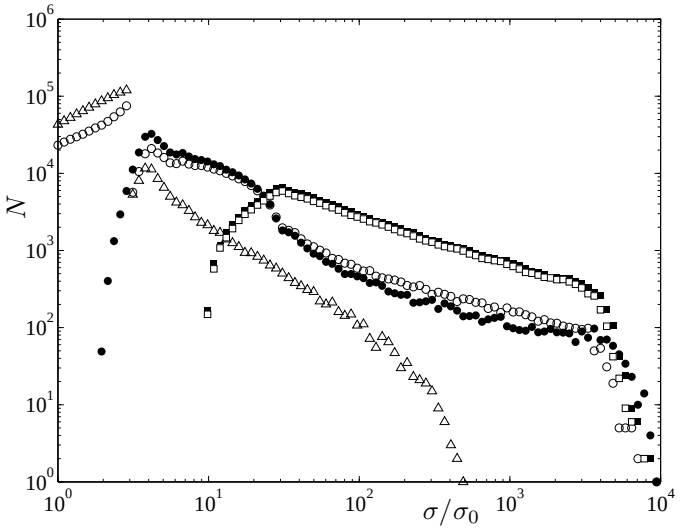

Figure 5: Number of collisions N per bin $[1.1^k\sigma_0, 1.1^{k+1}\sigma_0]$ over 10,000 time steps, which lead to a particle entering or leaving the bin. Triangles: contribution due to collisions with large particles; circles: contribution due to collisions with similar sized particles; squares: contribution due to collisions with small particles. Filled and open symbols correspond to number of particles entering and leaving the bin respectively.

are shown in Fig. 5. We notice that once collisions with small particles are counted at $\sigma/\sigma_0 = q$, with $q = 10$ in this figure, their contribution dominates almost immediately, and remains dominant for the entire inertial domain. We can also see that collisions with larger particles are only dominant in the forcing range $\sigma < 3\sigma_0$, and collisions with similar sized particles only marginally dominates in the intermediate regime for $3\sigma_0 < \sigma < 30\sigma_0$.

5 Self-similar solutions

KZ solutions studied in Sect. 3 are valid stationary solutions of the kinetic equation (5) in the systems modified by introduction of a local collision efficiency (e.g. using the model (11)). We have argued in Sect. 4 that without such an enforced locality the non-local interactions are dominant which results in a prediction for the steady state given in Eq. (18) and which is qualitatively confirmed in direct numerical simulations of the dynamics of particles.

However, both of these approaches assume homogeneity in space as well as a sink at large volumes (i.e. removing particles from the system when they reach a certain large size). These two conditions cannot be made realistically consistent because there is not a physical mechanism that could remove large particles from the bulk of the fluid.

Thus, it is more realistic to consider one of the following solutions:

- time-dependent, height-independent solutions without a sink
- height-dependent, time-independent solutions with a sink at a given height (i.e. for bubbles in water an interface with air at a given maximum value of z).

Both situations can be described by self-similar solutions of the kinetic equation (5). In the following derivations of the self-similar solutions we will suppose locality, in the sense that the dimensional analysis leading to the results supposes no dependence on the cut-off scales $\sigma_{\min}$ and $\sigma_{\max}$. Validity of the locality hypothesis will have to be examined *a posteriori*.

We will start by considering the particle model without forced locality, and later we will proceed by adding the effect of local collision efficiency followed by a super-local model leading to Burgers equation.

5.1 Height dependent solutions

Let us start with the analysis of the time-independent state. We look for a solution n that is self-similar in the sense that it verifies the scaling relation

$$n(\sigma, z) = z^{\alpha} h(z^{\beta}\sigma) \ . \tag{21}$$

To determine the exponents α and β we need two relationships. The first one is that Eq. (5) should give an equation on h as follows: introduce the self-similar variable $\tau = z^{\beta}\sigma$ to replace all occurrences of σ, then Eq. (5) can be written as

$$\tau^{2/3} z^{\alpha - \frac{2}{3}\beta - 1} [\alpha h(\tau) + \beta \tau h'(\tau)] = z^{2\alpha - \frac{7}{3}\beta} \int_0^{+\infty} \mathrm{d}\tau_1 \int_0^{+\infty} \mathrm{d}\tau_2 \, (T_{\tau 12} - T_{1\tau 2} - T_{2\tau 1}) \tag{22}$$

with the rate

$$T_{\tau 12} = \frac{c\kappa^{-4/3}\pi}{2} |\tau_2^{2/3} - \tau_1^{2/3}| (\tau_1^{1/3} + \tau_2^{1/3})^2 h(\tau_1) h(\tau_2) \delta(\tau - \tau_1 - \tau_2)$$

with $T_{1\tau 2}$ and $T_{2\tau 1}$ defined accordingly. We need to have equal powers of z on both sides, which gives

$$\alpha - \frac{2}{3}\beta - 1 = 2\alpha - \frac{7}{3}\beta \ .$$

The other relationship expresses constant flux of mass through a given height z. Since droplets of volume σ move with speed $u = u(\sigma)$, this flux is $\int n(z,\sigma)u\sigma \mathrm{d}\sigma$. With h and τ this becomes $\int z^{\alpha} h(\tau) z^{-2\beta/3} \tau^{2/3} z^{-\beta} \tau z^{-\beta} \mathrm{d}\tau$. The total power of z should be 0 for z to vanish from this expression, which gives us the second relationship

$$\alpha - \frac{8}{3}\beta = 0 \ .$$

Combining the two relations on α and β we find

$$\alpha = -\frac{8}{3} \ , \qquad\qquad \beta = -1 \ , \tag{23}$$

implying

$$n(\sigma, z) = z^{-8/3} h(\sigma/z) \ . \tag{24}$$

5.2 Time dependent solutions

Let us consider a self-similar distribution independent of z but dependent on time, of the form $n(\sigma,t) = \tilde{t}^{\alpha} h(\tilde{t}^{\beta}\sigma)$, where $\tilde{t} = t^* - t$ and t^* is a constant, the meaning of which will become clear shortly. The left hand side of Eq. (5) is replaced by $\partial_t n = \alpha \tilde{t}^{\alpha-1} h(\tilde{t}^{\beta}\sigma) + \beta \tilde{t}^{\alpha+\beta-1} \sigma h'(\tilde{t}^{\beta}\sigma)$. Upon introducing $\tau = \tilde{t}^{\beta}\sigma$, this becomes $\tilde{t}^{\alpha-1}[\alpha h(\tau) + \beta \tau h'(\tau)]$. The right hand side of Eq. (22) is unchanged except for replacing z by t. We thus obtain our first relationship

$$\frac{7}{3}\beta - \alpha = 1 \ . \tag{25}$$

One could think that the second relation should come from the conservation of mass $\int n(t,\sigma)\sigma \mathrm{d}\sigma = \int t^{\alpha} h(\tau) t^{-\beta} \tau t^{-\beta} \mathrm{d}\tau$. However, this condition is incorrect because the self-similar solution in this case gets realised only in a large–σ tail whereas most of the volume remains in the part which is not self-similar. This situation is typical of systems with finite capacity distributions, and it has been observed previously for the Alfvén wave turbulence [17] and for the Leith model of turbulence [18]. Thus, we have

$$n(\sigma,t) = (t^* - t)^{\alpha} h\left(\sigma (t^* - t)^{3(\alpha+1)/7}\right) \ .$$

As in the case of the Alfvén wave turbulence [17], it is very tricky to establish how to fix the second constant α but it can be found via numerical simulations of the kinetic equation (5).

The above self-similar solution describes creation of infinitely large particles in finite time, which rise with infinitely large velocities. Thus, no matter

how large our system is, close to the moment $t = t^*$ there will be particles that travel across the entire height in short time and, therefore, the z-independency assumption will fail. Note however that even close to the singularity moment $t = t^*$ the total volume fraction of such large particles remains small. We will study further details of such self-similar solutions using the "super-local" model in Sect. 7.2.

6 Locality of the self-similar solutions

Locality of interactions was assumed in the derivation of the self-similar solutions in Sect. 5.1. This does not need any further justification if a local collision efficiency like in Eq. (11) is used. However, in the case of cut-off free interaction kernels that assumption needs to be verified. In order to examine its validity we will now establish the asymptotic behavior, at small τ and at large τ, of the self-similarity function $h(\tau)$ introduced in Sect. 5. We shall make the hypotheses (to be verified below) that at very large τ the collision integral is dominated by contributions of the range of much smaller τ and, conversely, that at very small τ the collision integral is dominated by contributions of the range of much larger τ.

Let us start with the large τ case. Under the assumption for this range that we formulated in the previous paragraph, the distribution in this range evolves as in Eq. (15), i.e. in the z-dependent steady state we have

$$u\partial_z n = -c_1 \partial_\sigma (\sigma^{4/3} n) \ ,$$

which for $h(\tau)$ reduces to

$$\tau^{2/3}[\alpha h + \beta \tau h'] = -c_1 \tau^{1/3}[\frac{4}{3} h + \tau h'] \ .$$

Both sides are homogeneous in τ, but the left hand side is of degree $1/3$ higher than the right hand side, so its dominant contribution should cancel, leading to the asymptotics $h(\tau) \sim \tau^{-\alpha/\beta}$, and substituting values of α and β from Sect. 5.1 we get $h(\tau) \sim \tau^{-8/3}$. According to the results summarised in Table 1, such $-8/3$ tail corresponds on one hand to convergence of the collision integral at the large σ limit (as assumed in the self-similar solution) and, on the other hand, it corresponds to dominance of interactions with much smaller τ's as was assumed for derivations in this section.

Let us now consider the small τ range. As we have hypothesized above about this range, the dominant contribution to the collision integral now comes form the non-local interaction term with large particles, which for

small σ behaves as given in Eq. (16), leading to

$$u\partial_z n = -c_2 n \ ,$$

which for $h(\tau)$ reduces to

$$\tau^{2/3}[\alpha h + \beta\tau h'] = -c_2 h \ .$$

This can be solved explicitly and yields

$$h(\tau) = C_0 e^{\frac{3c_2}{2\beta}\tau^{-2/3}}\tau^{-\alpha/\beta} = C_0 e^{-\frac{3c_2}{2}\tau^{-2/3}}\tau^{-8/3} \ , \tag{26}$$

where $C_0 > 0$ is an integration constant and the last member has values of α and β substituted from Sect. 5.1. Thanks to the very strong stretched exponential decay of h at small τ the self-consistency of our hypotheses is straightforward to verify. At the same time, such fast decay at small τ ensures convergence of the collision integral at the $\sigma = 0$ limit.

We have therefore proven that our self-similar solutions are local. Note that this result is remarkable because, in contrast with the KZ solution, the locality property holds even without introducing a local collisional efficiency factor.

6.1 Numerical verification of the height dependent solutions

We have performed direct numerical simulations of the set of particles corresponding to the set-up where one should expect the self-similar behavior. Namely, we generate particles with distribution $n(\sigma) = \sin(\pi(\sigma - \sigma_0)/13)\sigma^{-2/3}$ and with vertical coordinate $0 < z < 0.5$ and we take them out of the system as soon as their center has crossed the surface at $z = 10$.

The results for the simulation with free merging are shown in Fig. 6. A rescaling to self-similar variables has already been done. We see that profiles at different z collapse, which confirms the self-similar character of our distribution with the self-similarity coefficients $\alpha = -8/3$ and $\beta = -1$ found in Sect. 5.1. Moreover, we observe that our profile at large τ is consistent with the $-8/3$ power law found above.

We have also performed computations with the forced locality model as given in Eq. (11) with $q = 2$. It comes to no surprise that the observed distribution is also self-similar (since the assumed locality has become even stronger). Naturally, the shape of the self-similar function $h(\tau)$ is now different. It is interesting that instead of the $-8/3$ scaling we now see a $-5/3$ slope. We will see in the next section that such a slope can be predicted by a

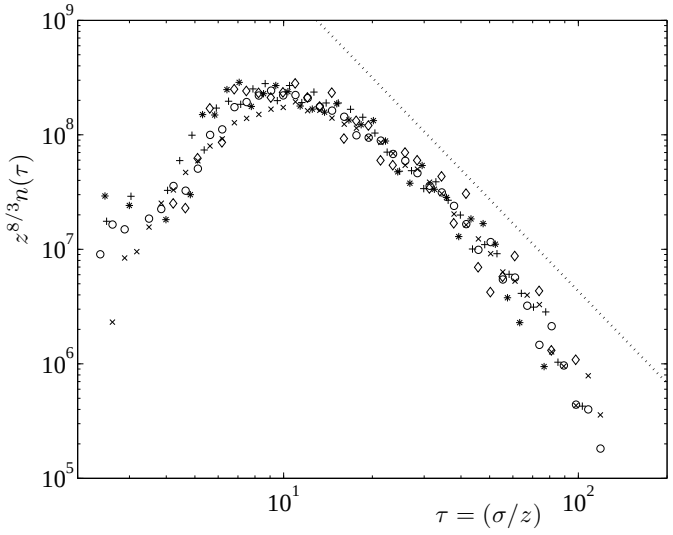

Figure 6: Distribution of particle volumes after 39,000 time steps for the situation without forced locality ("$q = \infty$"). The graph is presented in self-similar variables according to Eq. (24). The markers identify the spectrum for $z = 1.75$ ($\times$); $z = 3.75$ ($\circ$); $z = 5.75$ ($+$); $z = 7.75$ ($*$); $z = 9.75$ ($\Diamond$). The dotted slope represents a -8/3 power law.

"super-local" model where the integral kinetic equation (5) is replaced by an effective differential equation preserving the scalings of the local interactions. In the range of large τ we observe an exponential decay $h(\tau) \sim \exp(-b\tau)$ (where b is a constant), see Fig. 7. As will be shown below, these results are also predicted by a (regularised) "super-local" model.

7 Burgers equation for local interaction case

We will now study the systems with forced locality in greater detail by introducing a "super-local" model which preserves the essential scalings of the original kinetic equation (5), i.e.

$$\partial_t n + u\partial_z n = -\sigma^{-1}\partial_\sigma(\sigma^{13/3}n^2) \; . \tag{27}$$

Particularly, Eq. (27) has the same self-similarity exponents as those found in Sect. 5, in either case of height dependent or time dependent self-similar solutions. We see that on the right hand side n appears squared, making the equation reminiscent of Burgers equation. We are going to pursue this idea

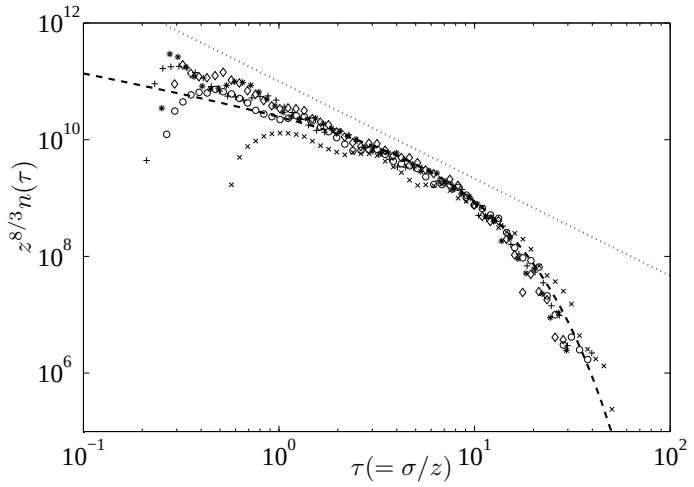

Figure 7: Distribution of particle volumes after 23,000 time steps for the forced locality situation with $q = 2$. The graph is presented in self-similar variables according to Eq. 24. The markers identify the spectrum for $z = 1.75$ ($\times$); $z = 3.75$ ($\circ$); $z = 5.75$ ($+$); $z = 7.75$ ($*$); $z = 9.75$ ($\Diamond$). The dotted slope represents a $-5/3$ power law, and the dashed curve shows $A\tau^{-2/3}\exp^{-\gamma\tau}$, made to fit the data at $\tau = 6$.

below, by studying the simpler cases of stationary solutions of this equation, either in z or in t.

7.1 Height dependent solutions

If we look for steady state in t only, then Eq. (27) reduces to

$$u\partial_z n = -\sigma^{-1}\partial_\sigma(\sigma^{13/3}n^2) \ .$$

We turn this into Burgers equation by introducing new variable s such that

$$\sigma = s^\lambda$$

and the new function

$$g(s) = As^\mu n(\sigma(s)) \ .$$

Then $\partial_z g = -(A\lambda)^{-1}s^{\mu-8\lambda/3+1}\partial_s(s^{13\lambda/3-2\mu}g^2)$. If we set $\mu - 8\lambda/3 + 1 = 0$ and $13\lambda/3 - 2\mu = 0$ and $(A\lambda) = 2$ then we recover Burgers equation:

$$\partial_z g = -g\partial_s g \ . \tag{28}$$

This happens for $\lambda = 2$, $\mu = 13/3$ and $A = 1$.

Conservation of total particle volume leads to the conservation of the integral $\int g(s)\mathrm{d}s$, and we deal with the usual Burgers dynamics even for the weak solutions (i.e. any regularisation of this equation should conserve the volume). In this case we get no finite-time singularity since A and λ are positive. We will use the analogy of (28) with Burgers equation and assume a discontinuity in our function g would be a shock in the equivalent Burgers system. The sawtooth shock can be seen to evolve such that at "time" z the shock is at $s_* \sim z^{1/2}$ and its height is $g_* \sim z^{-1/2}$ (hint: write $\mathrm{d}s_*/\mathrm{d}z = g_*/2$ and $s_* g_* = B$ where B is constant). For the original variables this gives $\sigma_* \sim z^{\lambda/2} = z$ and $n_0 \sim z^{-\mu/2} z^{-1/2} = z^{-8/3}$. One then sees that this solution is self-similar with the scaling we have found above. In fact

$$n(\sigma, z) = \begin{cases} z^{-8/3}(\sigma/z)^{-5/3} & \text{if } \sigma \le z, \\ 0 & \text{if } \sigma > z. \end{cases}$$

Remarkably, the $-5/3$ scaling of the self-similar function $h(\tau)$ is indeed observed in the numerical simulation of the particles with the forced locality collision efficiency, see Fig. 7. This fact indicates that, in spite of simplicity, the super-local model (27) is indeed quite efficient in predicting certain essential features of the particle kinetics. However, we have not observed any signature of a shock in our numerical results. Such a shock should be considered as an artifact of super-locality which is smeared out when a finite interaction range is allowed.

In fact, following the method exposed in Sect. 4.2 of ref. [2], it is also possible to obtain the asymptotic behaviour of $n(\sigma, z)$ for large $\tau = \sigma/z$ (see Sect. 5.1). This is beyond the reach of the Burgers model [1]. Following ref. [2] and using notation from our Sect. 5.1, we introduce the ansatz $h(\tau) \sim A\tau^{-\theta} e^{-\gamma\tau}$, where A, γ and θ are real constants, of which we shall only determine θ here. With this ansatz and using the flux formulation described in Appendix B, in particular Eqs. (29) and (30), we can write Eq. (22) as (note that we take the values of α and β from Eq. (23)):

$$\tau^{2/3}[-\tfrac{8}{3} A\tau^{-\theta} e^{-\gamma\tau} + (\theta - \gamma\tau) A\tau^{-\theta} e^{-\gamma\tau}] = \\ \tau^{-1}\partial_\tau \int_0^\tau \mathrm{d}\tau_1 \int_{\tau-\tau_1}^\infty \mathrm{d}\tau_2 \; K(\tau_1, \tau_2) A^2 \tau_1^{1-\theta} \tau_2^{-\theta} e^{-\gamma(\tau_1+\tau_2)}$$

The left hand side scales as $\tau^{2/3-\theta} e^{-\gamma\tau}$ while the right hand side can be seen to scale, for large τ, as $\tau^{4/3-2\theta} e^{-\gamma\tau}$ (in order to see this, note that

[1] Even if we added diffusive regularization to the Burgers model to account for not strict super-locality, we would get the incorrect $z^{-8/3}\exp(-\gamma\sigma/z)$ behaviour, where $\gamma > 0$ is some constant (see also Appendix B).

$e^{-\gamma(\tau_1+\tau_2)}$ attains its maximum over the integration domain along the segment $\tau_1+\tau_2=\tau$ with $\tau_1,\tau_2>0$ and becomes much smaller for $\tau_1+\tau_2-\tau \gtrsim \gamma^{-1}$, so that the *effective* integration domain is a band of width of order γ^{-1} around the segment $\tau_1+\tau_2=\tau$). In order for the two sides to have the same scaling we must have $\theta=2/3$. Then $h(\tau)\sim A\tau^{-2/3}e^{-\gamma\tau}$ and $n(\sigma,z)\sim Az^{-2}\sigma^{-2/3}e^{-\gamma\sigma/z}$.

7.2 Time dependent solutions

Let us now seek z–independent solutions of Eq. (27). In this situation the latter reduces to

$$\partial_t n = -\sigma^{-1}\partial_\sigma(\sigma^{13/3}n^2)\ .$$

We turn this into Burgers equation as above, introducing s and $g(s)$ as above. Then $\partial_t g = -(A\lambda)^{-1}s^{\mu-2\lambda+1}\partial_s(s^{13\lambda/3-2\mu}g^2)$. If we set $\mu-2\lambda+1=0$ and $13\lambda/3-2\mu=0$ and $A\lambda=2$ then we recover Burgers equation. This happens for $\lambda=-6$, $\mu=-13$ and $A=-1/3$.

In order to know what happens at shocks we need to know what quantity is conserved by evolution, even at shocks. We know that the original system conserves the volume $\int n\sigma \mathrm{d}\sigma$, which translates for g to conservation of $(\lambda/A)\int g(s)s^{2\lambda-\mu-1}\mathrm{d}s$, and since $2\lambda-\mu-1=0$ this simply means conservation of $\int g(s)\mathrm{d}s$. Thus once again we really deal with the usual Burgers dynamics.

If the initial distribution of n is peaked around σ_0 with height n_0 then the initial distribution of g is peaked around $s_0=\sigma_0^{1/\lambda}$ with height $g_0=As_0^\mu n_0$. It is convenient to suppose that the peak is of compact support, say between $\sigma_1<\sigma_2$, corresponding to $s_1>s_2$. Since n (the particle density) is positive but A is negative, g will be negative and shocks will move towards smaller s. The peak evolves to give a shock, which will have formed at some $s>s_2$. To good approximation we get a single sawtooth shock which moves towards 0 and reaches it in finite time, which for n means (since $\lambda<0$) that there is a finite-time singularity at infinite volume.

The important feature is that the shock in g will arrive at $s=0$ at some finite time t^*, and for t close to t^* its height and speed are approximately constant, say height g^* and position $s=\tilde{t}w^*$ where $\tilde{t}=t^*-t$. This translates for n to a jump of height $A^{-1}s^{-\mu}g^*=A^{-1}(\tilde{t}w^*)^{-\mu}g^*\propto\tilde{t}^{-\mu}$ at position $\sigma=s^\lambda\propto\tilde{t}^\lambda$. This is compatible with self-similarity $n(\sigma,t)=\tilde{t}^\alpha h(\tilde{t}^\beta\sigma)$ only for exponents $\alpha=-\mu=13$ and $\beta=-\lambda=6$, which satisfy the condition from Eq. (25).

Note also that, since g can be considered to be approximately constant behind the shock (i.e. towards large s) , the distribution of n behind the jump (i.e. towards small σ) is like $\sigma^{-13/6}$, which is a finite capacity power

law, as required by conservation of total initial finite mass.

Since self-similarity only appears in the tail of the distribution, and the tail has finite capacity, it is difficult to obtain good statistics in numerical simulations for this model. In the tail, there will be very large particles, but the void fraction will be large too, as $\int n\sigma d\sigma$ is constant, resulting in a sparse data set in the numerical simulation.

8 Concluding remarks

As we have seen, the very simple model in which particles move at their terminal velocity and merge upon collision appears to be very rich in features. For this model, we have derived the Smoluchowski kinetic equation (5) with a kernel for differential sedimentation.

First of all, we considered a setup analogous to one used in turbulence theory where small particles are produced and large particles are removed from the system with a wide inertial interval in between these source and sink scales. We obtained a KZ spectrum (Fig. 3) and showed that it is relevant for the systems with forced locality but irrelevant in the free-merging case. In the latter case we derived a model (17) in which the dominant interactions are non-local and we obtained its steady state solution in Eq. (18), which was verified with DNS (Fig. 4).

We have also considered self-similar solutions which are either height dependent or time dependent. This was done for both the kinetic equation (5) and for a model with "super-local" interactions (27). For the time dependent dynamics, we predicted a finite-time creation of infinitely large particles. The solutions for height dependent dynamics were verified with DNS. Although most particle distributions in the atmosphere are height dependent [5], the relevance of self-similarity in such distributions requires further study.

Our theoretical results were obtained from the kinetic equation (5) which is essentially a mean field approach. Thus, it is intriguing that such theoretical predictions in all considered situations agree well with the numerical simulations of the complete system. This suggests that the mean field assumption leading to the kinetic equation should be valid in the considered sedimentation model, and the origin of this could be addressed in the future with techniques of field theory and renormalization.

Finally, we have only considered very simple models either without the collision efficiency factor, or with a simple forced locality factor conform Eq. (11). Other forms of localizing kernels should be considered for more realistic situations.

Acknowledgements

We would like to thank Miguel Bustamante, Antti Kupiainen, Lian-Ping Wang and Oleg Zaboronski for helpful discussions and suggestions.

A Locality of power-law distributions

Power law distributions of the form $n(\sigma) \sim \sigma^\nu$ are important because they arise from the formal analysis of the KZ spectra, self-similar solutions, etc. However, some of such formal considerations implicitly use convergence of the collision integral on RHS of Eq. (5) which has the meaning of the interaction *locality*. Conversely, other derivations may assume *non-locality* i.e. that the evolution is dominated mostly by the interactions with the smallest or the largest particles in the system corresponding to the vicinities of the small-σ and the large-σ integration limits. Therefore, the conditions of convergence of the collision integral must be found, and this will be done in this appendix for a general distribution $n(\sigma) \sim \sigma^\nu$.

Introduce $f(\sigma_1, \sigma_2) = K(\sigma_1, \sigma_2) n_1 n_2$. Equation (5) may be expressed in terms of f as

$$\frac{\mathrm{d}}{\mathrm{d}t} n = \int_{\sigma_{\min}}^{\sigma/2} \mathrm{d}\sigma_1 f(\sigma_1, \sigma - \sigma_1) - \int_{\sigma_{\min}}^{\sigma_{\max}} \mathrm{d}\sigma_1 f(\sigma_1, \sigma) \ .$$

We can then split $\mathrm{d}n/\mathrm{d}t$ into two parts, which we shall call lower and upper contributions:

$$\frac{\mathrm{d}}{\mathrm{d}t} n = \left.\frac{\mathrm{d}}{\mathrm{d}t}\right|_< n + \left.\frac{\mathrm{d}}{\mathrm{d}t}\right|_> n$$

with

$$\left.\frac{\mathrm{d}}{\mathrm{d}t}\right|_< n = \int_{\sigma_{\min}}^{\sigma/2} \mathrm{d}\sigma_1 [f(\sigma_1, \sigma - \sigma_1) - f(\sigma_1, \sigma)]$$
$$\left.\frac{\mathrm{d}}{\mathrm{d}t}\right|_> n = -\int_{\sigma/2}^{\sigma_{\max}} \mathrm{d}\sigma_1 f(\sigma_1, \sigma) \ .$$

We start by analyzing the lower contribution, more specifically its convergence as $\sigma_{\min}$ goes to 0. For this the value of the integrand at $\sigma_1 \ll \sigma$ needs to be known. This can be approximated by the Taylor expansion

$$f(\sigma_1, \sigma - \sigma_1) - f(\sigma_1, \sigma) \sim \sigma_1 \partial_\sigma f(\sigma_1, \sigma) \ .$$

For small σ_1 we also have $f(\sigma_1, \sigma) \sim c\kappa^4 \pi \sigma^{4/3} n_1 n$ so we have

$$\left.\frac{\mathrm{d}}{\mathrm{d}t}\right|_< n \approx -c\kappa^4 \pi \left[\int_{\sigma_{\min}}^{\sigma/2} n_1 \sigma_1 \mathrm{d}\sigma_1\right] \partial_\sigma (\sigma^{4/3} n) \ .$$

	$\nu < -\frac{7}{3}$	$-\frac{7}{3} \leq \nu \leq -2$	$-2 < \nu$
upper	local	non-local	
lower	non-local		local

Table 1: Locality of interaction with small and large particles, as dependent on the scaling exponent of $n(\sigma)$ (compare Connaughton et al. [8]).

The interaction is local at small scales iff the integral above remains finite when $\sigma_{\min} \to 0$. This is equivalent to $\nu > -2$.

We now turn to the upper contribution, more specifically its convergence as $\sigma_{\max}$ goes to infinity. For this the value of the integrand at $\sigma_1 \gg \sigma$ needs to be known. In these asymptotics we have $f(\sigma_1, \sigma) \sim \sigma_1^{4/3} n_1 n$ and therefore

$$\left.\frac{\mathrm{d}}{\mathrm{d}t}\right|_{>} n \approx -n \int_{\sigma/2}^{\sigma_{\max}} n_1 \sigma_1^{4/3} \mathrm{d}\sigma_1 \ .$$

The interaction is local at large scales iff the integral above remains finite when $\sigma_{\max} \to \infty$. This is equivalent to $\nu < -7/3$.

We thus get the picture that for $\nu < -7/3$ the interaction is local at large scales but non-local at small scales. For $-7/3 \leq \nu \leq -2$ both ends are non-local. And for $\nu > -2$ interaction is non-local at large scales but local at small scales. In particular, we never have locality at both ends.

B Considerations on the flux

The flux $\Phi(\sigma)$ of volume going into particles of volume larger than σ can be obtained by the following consideration. The flux in question is the volume contained in particles of volumes smaller σ that merge during unit time with some particle to give a particle of volume larger than σ. Say one such particle has $\sigma_1 < \sigma$, then it can merge with any particle with σ_2 such that $\sigma_1 + \sigma_2 > \sigma$, i.e. $\sigma_2 > \sigma - \sigma_1$. Using the collision kernel K the above consideration is made formal as

$$\Phi(\sigma) = \int_0^{\sigma} \mathrm{d}\sigma_1 \int_{\sigma-\sigma_1}^{\infty} \mathrm{d}\sigma_2 \, \sigma_1 K(\sigma_1, \sigma_2) n(\sigma_1) n(\sigma_2) \ . \tag{29}$$

One readily verifies by direct computation (and a minor trick) that the right hand side of the kinetic equation (5) equals $-\sigma^{-1}\partial_\sigma \Phi(\sigma)$, so we have as we may expect

$$\sigma \frac{\mathrm{d}n(\sigma)}{\mathrm{d}t} = -\partial_\sigma \Phi(\sigma) \ . \tag{30}$$

We immediately remark two things about Φ. First, it is convergent at the lower bound ($\sigma_1 \to 0$) if and only if interaction with the small σ tail is local, and similarly it is convergent at the upper bound ($\sigma_2 \to \infty$) if and only if interaction with the large σ tail is local (compare with Appendix A).

The other remark is that $\Phi(\sigma)$ scales as $\sigma^{4/3+3+2\nu}$ (if n scales as σ^ν). Hence, for $\nu = -(4/3+3)/2 = -13/6$ we have $\partial_\sigma \Phi(\sigma) = 0$ and thus, from Eq. (30), $\sigma^{-13/6}$ is a stationary power law solution.

The next thing we do is Taylor expand n around $n(\sigma)$ in the expression (29) of the flux. Then to lowest (zeroth) order we get

$$\Phi(\sigma) = n(\sigma)^2 \int_0^\sigma \mathrm{d}\sigma_1 \int_{\sigma-\sigma_1}^\infty \mathrm{d}\sigma_2 \, \sigma_1 K(\sigma_1, \sigma_2) \ .$$

Since the integral above scales as $\sigma^{4/3+3}$, this can be written as

$$\Phi(\sigma) = C' \sigma^{4/3+3} n(\sigma)^2 \ ,$$

with $C' > 0$ (since $K \geq 0$), and substituting this into Eq. (30) we get an equation equivalent to Burgers equation (cf. Sect. 7).

Remark: perhaps one caveat is that the simple Taylor expansion proposed above doesn't seem to correspond to an expansion in some small parameter of the problem. One natural small parameter could be $q - 1$ from the definition (11) of the collision efficiency. But the expansion in $q - 1$ would be slightly more complex.

One can carry on this Taylor expansion and get terms of higher order, which will have more derivatives ∂_σ and higher powers of σ. In the "Burgers" coordinates introduced in Sect. 7, the same holds but with powers and derivatives in s. In particular to next order we get, in the setup of Sect. 7.2, $\partial_t g = -\partial_s (C_1 g^2 + C_2 s \partial_s g^2)$.

References

[1] Van Dongen, P. G. J. and Ernst, M. H. *Phys. Rev. Lett.* **54**(13), 1396–1399 (1985).

[2] Van Dongen, P. G. J. and Ernst, M. H. *J. Stat. Phys.* **50**(1/2) (1988).

[3] Lee, M. H. *Icarus* **143**, 74–86 (2000).

[4] Hunt, J. R. *J. Fluid Mech.* **122**, 169–185 (1982).

[5] Pruppacher, H. R. and Klett, J. D. *Microphysics of Clouds and Precipitation.* Kluwer Academic, (1997).

[6] Falkovich, G., Stepanov, M. G., and Vucelja, M. *J. Appl. Meteor. Clim.* **45**, 591–599 (2006).

[7] Jeffrey, D. J. *J. Atmos. Sci.* **38**, 2440–2443 (1981).

[8] Connaughton, C., Rajesh, R., and Zaboronski, O. *Phys. Rev. E* **69**, 061114 (2004).

[9] Pushkin, D. O. and Aref, H. *Phys. Fluids* **14**(2) (2002).

[10] Vinokurov, L. I., Kats, A. V., and Kontorovich, V. M. *J. Stat. Phys.* **38**(1/2) (1985).

[11] Landau, L. D. and Lifschitz, E. M. *Fluid Mechanics*. Pergamon Press, (1987).

[12] Clift, R., Grace, J. R., and Weber, M. E. *Bubbles, Drops, and Particles*. Academic Press, New York, (1978).

[13] Smoluchowski, M. *Z. Phys. Chem.* (1917).

[14] Valioulis, I. A., List, E. J., and Pearson, H. J. *J. Fluid Mech.* **143**, 387–411 (1984).

[15] Friedlander, S. K. *J. Meteor.* **17**, 479–483 (1960).

[16] Zakharov, V. E., L'vov, V. S., and Falkovich, G. *Kolmogorov Spectra of Turbulence*. Springer-Verlag, (1992).

[17] Galtier, S., Nazarenko, S. V., Newell, A. C., and Pouquet, A. *J. Plasma Phys.* **63**, 447 (2000).

[18] Connaughton, C. and Nazarenko, S. V. *Phys. Rev. Lett.* **92**, 044501 (2004).